

Large deviations of the dynamical activity in the East model: analysing structure in biased trajectories

Robert L. Jack

Department of Physics, University of Bath, Bath BA2 7AY, United Kingdom

Peter Sollich

Department of Mathematics, King's College London, Strand, London WC2R 2LS, United Kingdom

Abstract. We consider large deviations of the dynamical activity in the East model. We bias this system to larger than average activity and investigate the structure that emerges. To best characterise this structure, we exploit the fact that there are effective interactions that would reproduce the same behaviour in an equilibrium system. We combine numerical results with linear response theory and variational estimates of these effective interactions, giving the first insights into such interactions in a many-body system, across a wide range of biases. The system exhibits a hierarchy of responses to the bias, remaining quasi-equilibrated on short length scales, but deviating far from equilibrium on large length scales. We discuss the connection between this hierarchy and the hierarchical aging behaviour of the system.

1. Introduction

What is the probability that an extensive observable in a physical system has a value far from its average? Such questions are the subject of large-deviation theory [1], which provides a mathematical foundation for classical thermodynamics [2], and has more recently been applied to a variety of problems in non-equilibrium statistical mechanics [3, 4, 5, 6, 7, 8, 9, 10, 11]. Notable results in these non-equilibrium settings include analyses of fluctuation theorems [3]; exact results for exclusion processes and models of energy transport [4, 5, 6, 7, 8]; a proposed non-equilibrium counterpart of detailed balance in sheared systems [9]; and dynamical phase transitions in glassy systems [10, 11, 12, 13]. Here, we focus on trajectories in which an extensive measurement of dynamical activity [10, 14, 15] has a non-typical value, and we discuss how these trajectories can be characterised in terms of effective interactions [6, 8, 9, 16, 17, 18, 19, 20].

The nature of these effective interactions is important in interpreting measurements of large deviations in non-equilibrium systems. In particular, if the interactions are simple and short-ranged, one can interpret the large-deviation behaviour of the system in terms of its response to these short-ranged forces. In this situation, physical intuition and results from the existing literature can be very useful. However, there are at least some cases [4, 5, 13, 18] where long-ranged effective interactions appear, and lead to unusual new behaviour (for example, phase transitions to states with long-ranged order may appear in one-dimensional systems). In these cases, interpreting and analysing results for large deviations is more difficult. An example is given by the very stable “glass” states that appear in glassy model systems, when one considers large deviations of the dynamical activity [10, 11, 12, 21, 22] – it is not clear what effective interactions might be required to stabilise these states, and it is therefore difficult to understand what kinds of equilibrium or non-equilibrium protocols might be used to prepare them in the laboratory.

In this study, we present numerical and analytical results for the one-dimensional East model [23]. This simple spin system is an example of a kinetically constrained model [24, 25], where complex dynamical behaviour arises at low temperature, while all thermodynamic quantities remain very simple. The model has been studied extensively in the context of glassy systems [26, 27, 28], particularly within the theory of dynamical facilitation [29]. At low temperatures, it supports a very broad spectrum of time scales – this results in a range of glassy phenomena, and also considerable structure in the large deviation functions of the model. The model is useful for our purposes because its large deviations are quite rich and complex, but it is still tractable both numerically and analytically. We present several methods for characterising the effective interactions associated with large deviations in this model. The one-dimensional nature of the model greatly facilitates our analysis in this article, but we argue that our methods and general results have potential applicability for analysing effective interactions in a wide range of systems. Our results are the first to give direct insights into effective interactions over a range of biases in a many-body system, going beyond previously studied cases where

very few degrees of freedom were considered [8, 9, 16, 17, 19, 20], or the analysis was restricted to the limit of strong biasing [8].

The paper is organised as follows: In Section 2, we define the East model, the biased ensembles of trajectories that we study, and the observables that we use to characterise these ensembles. Section 3 gives an overview of the response to the bias, illustrated by numerical results. In Section 4, we use a linear-response (perturbative) formalism to analyse the effective interactions in the system, for small ν : the resulting physical picture is discussed in Section 5. Since strong long-ranged effective interactions appear even at the perturbative level, we then use non-perturbative variational schemes to estimate effective interactions (Sec. 6). Finally, we discuss implications of our results for more general systems in Sec. 7.

2. Model and ensemble definitions

2.1. East model

The one-dimensional East model [23, 24] has binary spins $n_i = 0, 1$ where the sites $i = 1 \dots N$ form a linear chain, with periodic boundaries. We identify $n_i = 1$ as the ‘up’ state and $n_i = 0$ as the ‘down’ state. The energy of the system has the simple form $E_0 = \sum_i n_i$, and spins flip with Glauber rates, subject to the kinetic constraint that spin i may flip only if spin $i - 1$ is in the ‘up’ state, $n_{i-1} = 1$. That is, spin i flips from $0 \rightarrow 1$ with rate $n_{i-1}c$, and from $1 \rightarrow 0$ with rate $n_{i-1}(1 - c)$, where $c = (1 + e^\beta)^{-1}$ is equal to the equilibrium fraction of ‘up’ spins, and β is the inverse temperature. We use the notation $\mathcal{C} = (n_1, n_2, \dots, n_N)$ to represent a configuration of the system.

We focus on the behaviour for small c (low temperature). At equilibrium, the dynamical behaviour of the system is hierarchical [26]: motion on a length scale ℓ requires the system to overcome an energy barrier of height

$$\alpha_\ell = \lceil \log_2 \ell \rceil. \quad (1)$$

That is, α_ℓ is the smallest integer greater than or equal to $\log_2 \ell$. Specifically, this is the energy barrier associated with relaxation of an up-spin that is a distance ℓ from the nearest up-spin to its left. At low temperature, the rates for such processes scale as

$$\tau_\ell = c^{\alpha_\ell} \sim e^{-\beta \alpha_\ell}, \quad \ell \lesssim 1/c. \quad (2)$$

The typical distance between up spins in the system at equilibrium is $1/c$: if one assumes that (2) applies on this length scale then one estimates the relaxation time of the system to be $\tau_{1/c} \sim e^{\beta^2 / \ln 2}$ [26, 27]. However, while this argument is persuasive, the bulk relaxation time at equilibrium in fact scales as $\tau_0 \sim e^{\beta^2 / (2 \ln 2)}$ [28]. The slower divergence arises because the simple argument above only considers the energy barrier of the most efficient path, but neglects speed-ups arising from the availability of many paths. These become significant for $\ell \approx 1/c$. For length scales ℓ larger than $1/c$, the system relaxes by undergoing approximately $c\ell$ successive events, each operating on a length scale of order $1/c$, and taking a time of order τ_0 : hence we expect $\tau_\ell \sim c\ell\tau_0$.

2.2. Large deviations

To investigate large deviations in the East model, we begin with its master equation:

$$\partial_t P(\mathcal{C}, t) = -r(\mathcal{C})P(\mathcal{C}, t) + \sum_{\mathcal{C}' \neq \mathcal{C}} W(\mathcal{C} \leftarrow \mathcal{C}')P(\mathcal{C}', t), \quad (3)$$

where $W(\mathcal{C} \leftarrow \mathcal{C}')$ is the transition rate from \mathcal{C}' to \mathcal{C} and

$$r(\mathcal{C}) = \sum_{\mathcal{C}' \neq \mathcal{C}} W(\mathcal{C}' \leftarrow \mathcal{C}) \quad (4)$$

is the escape rate from configuration \mathcal{C} . Writing $|P(\mathcal{C}, t)\rangle = \sum_{\mathcal{C}} P(\mathcal{C}, t)|\mathcal{C}\rangle$, the master equation is $\partial_t |P(\mathcal{C}, t)\rangle = \mathbb{W}|P(\mathcal{C}, t)\rangle$ where \mathbb{W} is the ‘master operator’ (or generator). Using a spin- $\frac{1}{2}$ basis for the configurations of the system, one has [10]

$$\mathbb{W} = \sum_i \hat{n}_{i-1} [(1-c)\sigma_i^- + c\sigma_i^+ - (1-2c)\hat{n}_i - c], \quad (5)$$

where $\hat{n}_i|\mathcal{C}\rangle = n_i|\mathcal{C}\rangle$ gives the state of spin i in configuration \mathcal{C} , while the σ_i^\pm are raising and lowering operators for spin i . (Explicitly, if we write a configuration with $n_i = 0$ or $n_i = 1$ as $|\cdots 0 \cdots\rangle$ or $|\cdots 1 \cdots\rangle$ respectively, then the operators act as $\sigma_i^+|\cdots 0 \cdots\rangle = |\cdots 1 \cdots\rangle$ and $\sigma_i^-|\cdots 1 \cdots\rangle = |\cdots 0 \cdots\rangle$, while $\sigma_i^+|\cdots 1 \cdots\rangle = 0 = \sigma_i^-|\cdots 0 \cdots\rangle$.)

Large deviations of the dynamical activity in the East model were first considered in Ref. [32] and later in [10, 33]. Consider a trajectory of length (‘observation time’) t_{obs} , which contains a total of K configuration changes. At equilibrium, K has a probability distribution $P_0(K)$: if the system size N and the observation time t_{obs} are large then the central limit theorem implies that the variance and mean of K both scale as Nt_{obs} . Thus, $P_0(K)$ becomes sharply peaked as $N, t_{\text{obs}} \rightarrow \infty$. Nevertheless, one may still consider trajectories with non-typical values of K . One expects

$$P_0(K) \simeq e^{-Nt_{\text{obs}}\pi_K(k)}, \quad (6)$$

where $k = K/(Nt_{\text{obs}})$ and $\pi_K(k)$ is a ‘spacetime free energy’ or ‘rate function’ that determines the probability of particular values of K [30].

In practice, it is convenient to follow an equivalent route, concentrating not on $\pi_K(k)$ but on its Legendre transform $\psi_K(s) = \min_k [sk + \pi_K(k)]$. To achieve this, one defines (as in Ref. [10]) a probability distribution over trajectories:

$$\text{Prob}[\mathcal{C}(t), s] = \text{Prob}[\mathcal{C}(t), 0] \cdot \frac{e^{-sK}}{\langle e^{-sK} \rangle_0}, \quad (7)$$

where $\mathcal{C}(t)$ represents a trajectory of the system and K denotes its activity, while the parameter s biases the equilibrium distribution $\text{Prob}[\mathcal{C}(t), 0]$, favouring trajectories with non-typical values of K . The notation $\langle \cdot \rangle_0$ indicates an equilibrium average.

Following [10, 11], we refer to the probability distribution $\text{Prob}[\mathcal{C}(t), s]$ as an ‘ s -ensemble’. In the following, we use $\langle \cdot \rangle_s$ to represent an average with respect to this distribution. Standard arguments based on equivalence of ensembles indicate that averages with respect to $\text{Prob}[\mathcal{C}(t), s]$ are equivalent to averages over trajectories with fixed values of K (see also [20]). In the long time limit, the free energy $\psi_K(s)$ may

be obtained from $\langle e^{-sK} \rangle_0 \simeq e^{-N t_{\text{obs}} \psi_K(s)}$ [31]. We will consider averages of one-time quantities (like $\langle n_i(t) \rangle_s$), as well as quantities that depend on the whole trajectory (like $\langle K \rangle_s$). Averages of one-time quantities are independent of the time t at which they are evaluated, except for initial and final ‘transient’ regimes near $t = 0$ and $t = t_{\text{obs}}$. Unless otherwise stated, we evaluate all one-time quantities at time $t = t_{\text{obs}}/2$, which is representative of the steady-state regime.

As discussed in [10], properties of s -ensembles in the East model may be obtained by analysis of the operator

$$\mathbb{W}_K(s) = \sum_i \hat{n}_{i-1} [e^{-s}(1-c)\sigma_i^- + e^{-s}c\sigma_i^+ - (1-2c)\hat{n}_i - c]. \quad (8)$$

The largest eigenvalue of $\mathbb{W}_K(s)$ is equal to $-N\psi_K(s)$. Let the left and right eigenvectors corresponding to this eigenvalue have elements $u_{\mathcal{C}}$ and $v_{\mathcal{C}}$ respectively, normalised such that $\sum_{\mathcal{C}} u_{\mathcal{C}} v_{\mathcal{C}} = 1$. Then the steady-state probability of configuration \mathcal{C} within the s -ensemble is $p_{\mathcal{C}} = u_{\mathcal{C}} v_{\mathcal{C}}$.

The large deviations of K are closely related to those of the ‘time-integrated escape rate’ [10],

$$R[\mathcal{C}(t)] = \int_0^{t_{\text{obs}}} dt r(\mathcal{C}(t)), \quad (9)$$

where $r(\mathcal{C})$ was defined in (4), above. By analogy with (7), we define a ‘ ν -ensemble’ by

$$\text{Prob}[\mathcal{C}(t), \nu] = \text{Prob}[\mathcal{C}(t), 0] \cdot \frac{e^{\nu R}}{\langle e^{\nu R} \rangle_0}. \quad (10)$$

The properties of this ensemble may be obtained from the operator

$$\mathbb{W}_R(\nu) = e^s \mathbb{W}_K(s), \quad e^s = 1 - \nu. \quad (11)$$

The largest eigenvalue of $\mathbb{W}_R(\nu)$ is therefore $-N\psi_R(\nu)$ with $\psi_R(\nu) = e^s \psi_K(s)|_{e^s=1-\nu}$, and the eigenvectors associated with this eigenvalue are the same $u_{\mathcal{C}}$ and $v_{\mathcal{C}}$ found by diagonalising $\mathbb{W}_K(s)$. We use $\langle \cdot \rangle_{\nu}$ to represent averages with respect to $\text{Prob}[\mathcal{C}(t), \nu]$. From (11), it follows that the ν -ensemble and the s -ensemble contain the same information (at least for $\nu < 1$).

Since the dynamics of the East model obeys detailed balance, and the activity K is time-reversal symmetric, the operator $\mathbb{W}_K(s)$ may be symmetrised [10] as $\mathbb{H}_K(s) = e^{\beta \sum_i \hat{n}_i/2} \mathbb{W}_K(s) e^{-\beta \sum_i \hat{n}_i/2}$; the same transformation also symmetrises $\mathbb{W}_R(\nu)$. It follows [18] that both s -ensembles and ν -ensembles may be described by ‘auxiliary Markov models’ that obey detailed balance with respect to the distribution $P_s(\mathcal{C}) \propto u_{\mathcal{C}}^2 e^{-\beta \sum_i n_i}$. Hence, we write

$$u_{\mathcal{C}} = e^{-\Delta V_{\mathcal{C}}/2} \quad (12)$$

and interpret $\Delta V_{\mathcal{C}}$ as an ‘effective potential’ that acts to drive the system into the ν -ensemble (see also [6]). If $\Delta V_{\mathcal{C}}$ is known then steady state averages of one-time quantities may be obtained by the methods of equilibrium statistical mechanics, using the energy function $\beta E(\mathcal{C}) = \beta \sum_i n_i + \Delta V_{\mathcal{C}}$. The main purpose of this paper is to investigate the ‘effective potential’ $\Delta V_{\mathcal{C}}$ that describes the ν -ensemble for the East model.

2.3. Observables and correlation functions

As well as the effective potential ΔV_C , which fully describes the biased state, we also consider several simpler observables that provide insight into the response to the bias. These include the mean escape rate,

$$r(\nu) = \frac{1}{Nt_{\text{obs}}} \langle R \rangle_\nu, \quad (13)$$

which indicates how strong the bias ν must be, in order to produce a particular deviation of R from its average. From the definition of the dynamical free energy $\psi_R(\nu)$ as the long-time limit of $-1/(Nt_{\text{obs}}) \ln \langle e^{\nu R} \rangle_0$ it follows that $r(\nu) = -\psi'_R(\nu)$. The derivative $\chi_R(\nu) = r'(\nu) = -\psi''_R(\nu)$, then indicates the size of the fluctuations of R , via

$$\begin{aligned} \chi_R(\nu) &= \frac{1}{Nt_{\text{obs}}} [\langle R^2 \rangle_\nu - \langle R \rangle_\nu^2] \\ &= \frac{1}{Nt_{\text{obs}}} \sum_{ij} \int_0^{t_{\text{obs}}} dt dt' \langle \delta r_i(t) \delta r_j(t') \rangle_\nu, \end{aligned} \quad (14)$$

where

$$r_i = (1 - c)n_{i-1}n_i + cn_{i-1}\bar{n}_i \quad (15)$$

is the escape rate at site i . We use the notation $\bar{n}_i = 1 - n_i$ and $\delta O = O - \langle O \rangle$.

To characterise spatial correlations in the biased state, we define

$$C(x) = \langle \delta n_i \delta n_{i+x} \rangle_\nu. \quad (16)$$

At equilibrium, $C(x) = c(1 - c)\delta_{x,0}$, since the energy function of the system lacks any interactions between spins. However, the presence of a non-zero effective potential ΔV_C modifies $C(x)$, which then provides a simple characterisation of response to the bias.

Finally, an observable that is very useful for probing the structure of biased states is a probability distribution for domain sizes, denoted by $p(d)$. Here, each domain consists of a single up-spin and all the down-spins to its right, up to (but not including) the next up-spin. This definition is slightly different from the natural definition of domains in (for example) a one-dimensional Ising model, where a block of adjacent up spins would form a single domain: in our case, each up spin forms its own separate domain. Our definition is motivated by the fact that up spins are typically quite rare, and the spacing between these spins is a dominant factor in determining dynamical behaviour. More formally, we define observables $U_{i,i+r}$ and $D_{i,i+r}$ which are equal to unity if spins i to $i + r$ are all up (U), or all down (D), and zero otherwise. That is,

$$U_{i,i+r} = \prod_{j=i}^{i+r} n_j, \quad D_{i,i+r} = \prod_{j=i}^{i+r} \bar{n}_j. \quad (17)$$

In this notation, the domain size distribution is

$$p(d) = \frac{\langle n_i \cdot D_{i+1,i+d-1} \cdot n_{i+d} \rangle_\nu}{\langle n_i \rangle_\nu}. \quad (18)$$

At equilibrium, one has the distribution $p^0(d) = c(1 - c)^{d-1}$.

2.4. Range of effective interactions

For a finite system, it is always possible to write the eigenvector $u_{\mathcal{C}}$ as $e^{-\Delta V_{\mathcal{C}}/2}$, as in (12). However, the question of whether $\Delta V_{\mathcal{C}}$ has the features expected of a “physical” potential is a subtle one. For spin models, Ising-like potentials such as $V_{\mathcal{C}} = \mu \sum_i n_i - \epsilon \sum_i n_i n_{i+1}$ are familiar, but $\Delta V_{\mathcal{C}}$ may also contain two-body interaction terms like $n_i n_{i+x}$ of larger range x , or many-body terms like $n_i n_{i+1} n_{i+2}$, which is a three-body interaction of range 2. While these are less familiar in physical situations, we show below that $\Delta V_{\mathcal{C}}$ for the East model with $\nu > 0$ must contain a combination of such terms with unbounded range (up to the system size), and we argue that this behaviour can be expected more generally. Specifically, if the longest range interaction term in $\Delta V_{\mathcal{C}}$ has range $B - 1$ then the domain size distribution $p(d)$ must decay exponentially for $d > B$ (a derivation is given in Appendix A.2). In the following, we will present numerical and analytic evidence that for $\nu > 0$, $p(d)$ decays faster than exponentially at large d , indicating the effective potential contains *long-ranged interactions*: that is, no effective potential with interactions of bounded range can fully represent $\Delta V_{\mathcal{C}}$ as the system size $N \rightarrow \infty$. In this sense, the states that occur for $\nu > 0$ in these systems are qualitatively more complex than those of classical spin models at equilibrium. This is part of the reason for the rich behaviour that has been observed in the large deviations of such systems, even in one dimension [4, 5, 7, 10].

We also note in passing that effective potentials similar to $\Delta V_{\mathcal{C}}$ have been considered in the mathematical literature. For example, instead of considering configurations \mathcal{C} within long trajectories, one can consider the configuration of a single (two-dimensional) lattice plane, within a three-dimensional Ising model [34]. Similar questions also arise within the renormalisation group [35]. The main question that has been addressed there is whether the effective interactions are “Gibbsian”: that is, whether $\Delta V_{\mathcal{C}}$ is a “reasonable Hamiltonian” in the sense defined rigorously in [35]. (The idea is based on considerations of locality, in the sense that the interactions encoded by $\Delta V_{\mathcal{C}}$ should decay sufficiently quickly with interaction range [35].) In the following, we focus on the specific interactions that we find within the East model: whether these interactions are Gibbsian or not is a question that we postpone for later studies.

3. Overview of response to bias, and numerical results

This Section introduces the most important features of the response of the East model to the bias ν . We present numerical results that illustrate the structure that develops when the bias ν is applied, and we also discuss two concepts that are important for interpreting this structure: the notion of ‘quasiequilibrium’, and the existence of scaling behaviour at small c .

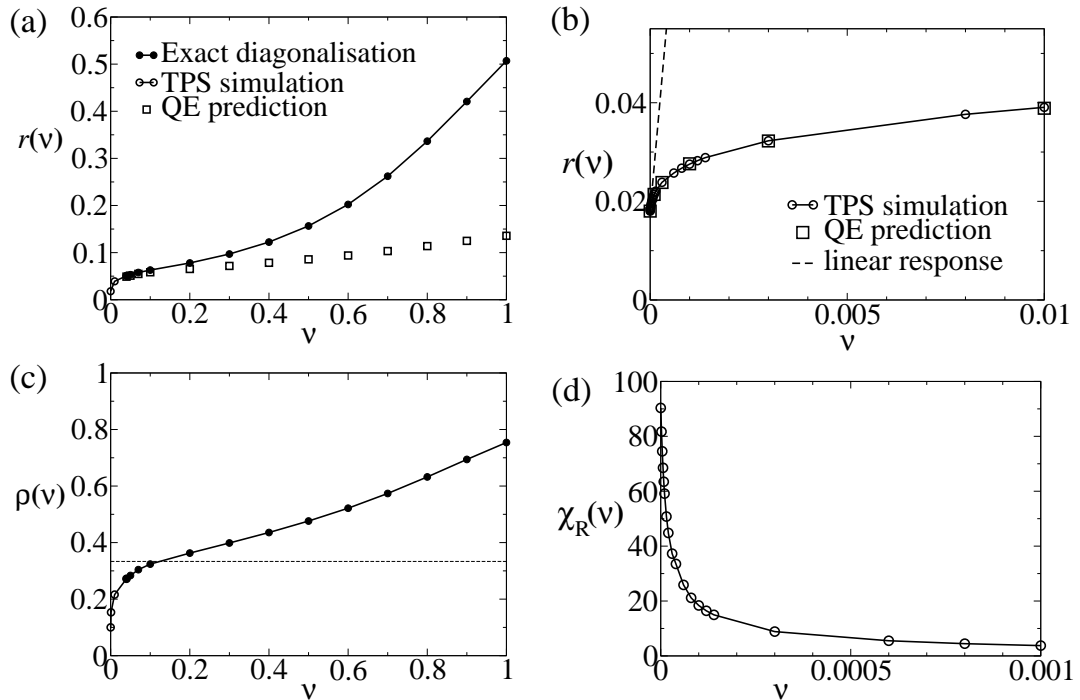


Figure 1. The mean escape rate $r(\nu)$, up-spin density $\rho(\nu) = \langle n_i \rangle_\nu$, and the susceptibility $\chi_R(\nu)$, in the East model for $c = 0.1$. (a) Mean escape rate $r(\nu)$ for the range $0 < \nu < 1$ (corresponding to $-\infty < s < 0$ in the s -ensemble). This is compared with the prediction of the quasiequilibrium (QE) assumption (20). (b) Mean escape rate $r(\nu)$ for small ν . The QE assumption holds quite accurately. (c) Mean up-spin density $\rho(\nu)$. The dashed line indicates $\rho(\nu) = \frac{1}{3}$, which is the predicted density in the limit $c \ll \nu \ll 1$ (see text). (d) The susceptibility $\chi_R(\nu)$, for small ν . In all panels, solid circles show data from exact diagonalisation of the operator $\mathbb{W}_R(\nu)$ and open circles are data from transition path sampling (TPS) [36]. The system sizes are $N = 14$ (exact diagonalisation), $N = 32$ (TPS for $\nu \geq 0.01$) and $N = 64$ (TPS for $\nu < 0.01$).

3.1. Mean activity and susceptibility

The ν -ensemble may be sampled numerically using transition path sampling (TPS) [36]: we follow the methods described in [11, 13]. For small systems (at least up to $N = 14$) one may also diagonalise the operator $\mathbb{W}_R(\nu)$ exactly, and obtain ΔV_c directly from its eigenvectors. (It is convenient to first symmetrise the operator, as described in Section 2.)

Fig. 1 shows numerical results for the average escape rate in the ν -ensemble, and the associated susceptibility $\chi_R(\nu)$. For the exact diagonalisation, we show results for $N = 14$: we also analyzed the case $N = 12$ for which the results agree to within the symbol sizes, indicating that finite-size effects are small. In the TPS calculations, we vary t_{obs} according to the state point, to ensure convergence of the large- t_{obs} limit. We have not carried out a detailed analysis of finite size effects but we do ensure that systems are significantly larger than almost all domains that appear at each state point

(see discussion in future sections). We therefore expect finite size effects to be small in these cases too.

In Fig. 1(d), it is striking that $\chi_R(\nu)$ is large as $\nu \rightarrow 0$, so that the average escape rate $r(\nu)$ responds strongly to the bias ν . We emphasise however that this susceptibility is finite even as $N, t_{\text{obs}} \rightarrow \infty$. To show this, we use a property of the East model at equilibrium. Suppose that A and B are two observables that depend on the spins only in non-overlapping regions of the system. By this we mean that all the spins that A depends on are to the left of those in B , or vice versa. Then one has

$$\langle \delta A(t) \delta B(t') \rangle_0 = 0. \quad (19)$$

This result [24] follows from the directionality of the kinetic constraint in the East model, which means that information can only flow from left to right in the system. Causality then implies that the state of spins with $j > i$ at time t cannot affect the behaviour of spin i for any $t' > t$. In fact, this property holds both at equilibrium and during relaxation towards equilibrium, which is sufficient to prove that a restricted version of (19) holds both in and out of equilibrium. That is, (19) holds both in equilibrium and out of equilibrium as long as $t' > t$ and observable B is localised to the left of observable A . At equilibrium, time-reversal symmetry then implies that (19) holds for all t and t' .

Combining Eqs (15,19), one finds that $\langle \delta r_i(t) \delta r_j(t') \rangle_0 = 0$ for $|i - j| > 1$. And for any i, j with $|i - j| \leq 1$, the finite spectral gap [28] of the operator \mathbb{W} means that $\langle \delta r_i(t) \delta r_j(t') \rangle_0$ decays exponentially for long times. Thus, the combined integral and sum in (14) leads to a finite result, at $\nu = 0$. We also note that the ratio $r(0)/\chi_R(0)$ sets a natural scale for ν : the strength of bias required to introduce an $O(1)$ relative change in activity. From (14), this can be estimated to be of the order of τ_0^{-1} where τ_0 is the equilibrium relaxation time, of the order of the inverse spectral gap. In fact, the bias ν has a hierarchy of natural scales, of which this is just the smallest. We return to this point in later Sections.

3.2. Quasiequilibrium condition

One effect of the parameter ν is to bias the system away from its equilibrium state. However, an important observation for interpreting the results of this article is that some degrees of freedom in the East model remain ‘quasiequilibrated’ in the presence of the bias, at least as long as c is small and ν is not too large. This means that even if configurations of the system have probabilities far from their equilibrium values, *ratios* of probabilities for some configurations may be almost unaffected by the bias. In other words, one may identify pairs of states for which $\Delta V_{\mathcal{C}} - \Delta V_{\mathcal{C}'}$ is small, even if the absolute values of the effective potential are large.

To illustrate this situation, suppose that spin i is “facilitated” in the East model (that is, $n_{i-1} = 1$). Then spin i will flip on a relatively rapid time scale of order c^{-1} . At low temperatures (small c), it is likely that spin $i - 1$ will flip only on a much slower time scale. In this case, spin i typically flips many times before spin $i - 1$ flips at all. Holding all other spins in the system constant, one then compares configuration \mathcal{C}

(where $n_i = 0$), with configuration \mathcal{C}' (where $n_i = 1$). Regardless of whether the system was initially in \mathcal{C} or \mathcal{C}' , the rapid flips of spin i mean that the ratio of probabilities of these configurations after a time of order $1/c$ will be very close to $c/(1-c)$, which is equal to their ratio at equilibrium. (Here we exploit the smallness of ν to neglect the effects of the bias on local spin flips.) It follows that $\langle n_{i-1}n_i \rangle_\nu \approx \langle n_{i-1} \rangle_\nu c$. To the extent that this holds, one has from (15) that

$$\langle r_i \rangle_\nu \approx 2c(1-c)\langle n_i \rangle_\nu, \quad r(\nu) \approx 2c(1-c)\langle \rho \rangle_\nu \quad (20)$$

where $\rho = N^{-1} \sum_i n_i$. These relations indicate that the escape rate and the density of up spins in the biased ensemble are tightly correlated for the East model, as found numerically in [32, 37]

Fig. 1 confirms that the quasiequilibrium relation (20) does hold quite accurately for $\nu \lesssim c$. For larger ν , quasiequilibrium breaks down: the response for $\nu = O(1)$ changes in character, resulting in a steady increase in the escape rate but departure from quasiequilibrium. For $c \ll \nu \ll 1$, we expect a plateau in $r(\nu)$, which represents a quasiequilibrium state with $\langle n_i \rangle_\nu \approx \frac{1}{3}$ (see Sec. 5 below). The data in Fig. 1(c) are consistent with such a regime, although numerical limitations prevent us from obtaining results at smaller c , which would allow this hypothesis to be tested further. In the regime $\nu > 1$, the function $r(\nu)$ increases smoothly, finally saturating in the state with all up spins as $\nu \rightarrow \infty$ (data not shown).

The quasi-equilibrium argument above can also be applied to individual configurations, not just averages over configurations. It then says that while a spin at site $i-1$ is up ($n_{i-1} = 1$), it causes the escape rate of the configuration $R = \sum_j r_j$ (or more precisely its contribution from site i) to be higher by $2c(1-c) - 2c^2(1-c) = 2c(1-c)^2 \approx 2c$ than the equilibrium average of $2c^2(1-c)$ per site. Conversely, a down-spin lowers the escape rate, changing it by $-2c^2(1-c) \approx -2c^2$.

3.3. Spatial correlations

We now turn to spatial structure in the ν -ensemble. Our overall aim is to arrive at a representation of the effective potential $\Delta V_{\mathcal{C}}$, but we begin by considering simple measures of order, to gain an overview of the structure of the system.

In Fig. 2(a), we show the two-point correlation function $C(x)$ defined in (16). For $\nu > 0$, up spins appear to ‘repel’ each other: the probability of finding two up-spins close together is suppressed, with respect to the value for independently fluctuating spins found at equilibrium. For $\nu \gtrsim 10^{-3}$, one observes oscillations in $C(x)$: just beyond the range of the short-ranged ‘repulsive’ correlations is a ‘nearest neighbour peak’ where up spins are more likely to be found.

The correlations that are apparent in $C(x)$ remain quite weak as ν increases, in stark contrast to the large changes in $r(\nu)$ and $\chi_R(\nu)$ shown in Fig. 1. A more revealing measurement of the system’s structure in the ν -ensemble is to consider the distribution of domains of down spins $p(d)$ as defined in (18). Figs. 2(b,c) show that there is considerable structure in the tails of $p(d)$. From a physical point of view, the key

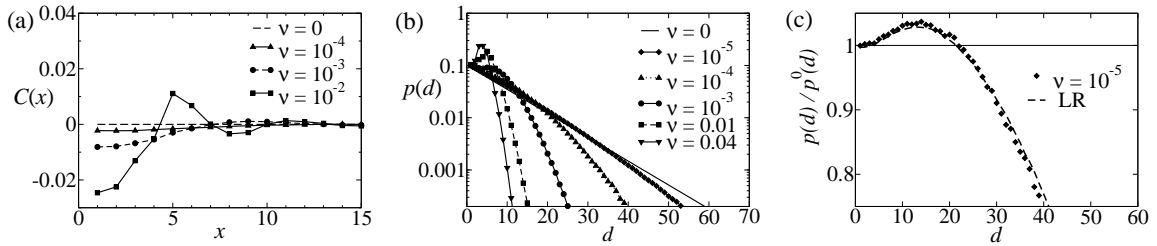


Figure 2. Spatial structure in the East model for $c = 0.1$. (a) Correlation function $C(x)$. (b) Distribution of domain sizes $p(d)$. (c) Plot of $p(d)/p^0(d)$ for $\nu = 10^{-5}$, where $p^0(d)$ is the equilibrium distribution of domain sizes. The dashed line shows the prediction of linear response theory (LR), obtained via the fluctuation formula (22), by numerical evaluation of the relevant equilibrium correlation function.

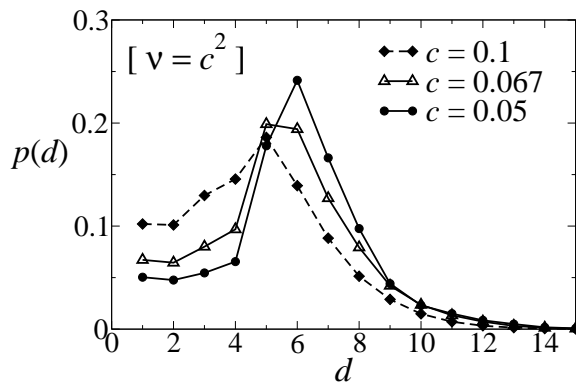


Figure 3. Domain distribution $p(d)$, for $\nu = c^2$ and varying c . This distribution is peaked around an emergent length scale and the peak becomes sharper as c is reduced, indicating that this length scale can be associated with the limit of small- c , given $\nu = c^2$. In this limit, scaling arguments (see Sec. 5 below) predict that $p(d) = O(c)$ for $d \leq 4$ while $p(d)$ has a positive limit for $d \geq 5$. This is consistent with the data, although the system is still quite far from the small- c limit.

aspects of $p(d)$ are that the distribution narrows as ν increases, with large domains being strongly suppressed, while small domains (for example $d = 1$ and $d = 2$) are only weakly affected. The probability associated with the larger domains is transferred to intermediate domain lengths which become increasingly common, eventually leading to a peak in $p(d)$ at an emergent length scale $d^* > 1$. Since the relaxation times for the largest domains are longest, then (14) indicates that the suppression of large domains is directly linked with the suppression of the susceptibility $\chi_R(\nu)$ as ν is increased [recall Fig. 1 and Eq. (14)]. We also note in passing that the arguments leading to the quasiequilibrium condition (20) predict $p(d = 1) = c$, which holds quite accurately in Fig. 2(b). In the following Sections, we will concentrate on $p(d)$ as an observable that reveals the dominant correlations within the biased steady state.

3.4. Scaling behaviour

It is well-known that length and time scales are intrinsically connected in the East model, both at equilibrium and in the aging behaviour [26]. Indeed, it is clear from (2) that the model obeys scaling relations in the limit $c \rightarrow 0$, where both length and time scales diverge. In the presence of the bias ν , it will be useful to consider limits where both c and ν go to zero together: we typically fix $\nu = c^b$ and then take $c \rightarrow 0$. Fig. 3 shows numerical results with $\nu = c^2$, as c is varied. One sees that $p(d)$ develops a peak at an emergent length scale, and that this peak becomes increasingly well-defined as c is reduced. In the next Section, use a perturbative scheme to analyse this kind of behaviour in more detail. This leads to a physical picture that we outline in Section. 5, where we identify the limit of $c \rightarrow 0$ at $\nu = c^b$ with a sharply-defined b -dependent length scale.

4. Linear response theory

At first order in ν , we can obtain a formula for the effective potential $\Delta V_{\mathcal{C}}$ using linear response theory (perturbation theory about the equilibrium state). Consider a one-time quantity f , and its average $\langle f \rangle_{\nu}$. For small ν , Eq. (10) gives

$$\langle f \rangle_{\nu} = \langle f \rangle_0 + \nu \langle \delta f \delta R \rangle_0 + O(\nu^2). \quad (21)$$

We note that $\langle \delta f \delta R \rangle_0 = \langle f \delta R \rangle_0$: it is sometimes convenient to use this latter form in the following. In addition, the first-order term in (21) may be written as

$$\delta \langle f \rangle = \nu \sum_j \int_0^{t_{\text{obs}}} dt \langle \delta f(t') \delta r_j(t) \rangle_0. \quad (22)$$

where we used (15), and we evaluate f at $t' = t_{\text{obs}}/2$ to avoid transient regimes, as discussed above. For large enough t_{obs} (and using time-reversal symmetry at equilibrium), this may also be written as [10]

$$\delta \langle f \rangle = 2\nu \sum_j \int_0^{\infty} dt \langle \delta f(0) \delta r_j(t) \rangle_0. \quad (23)$$

To obtain $\Delta V_{\mathcal{C}}$, we take $f = e_{\mathcal{C}}$ to be an indicator function, which has a value of unity if the system is in configuration \mathcal{C} , and zero otherwise. One finds

$$\begin{aligned} \Delta V_{\mathcal{C}} &= -\frac{\delta \langle e_{\mathcal{C}} \rangle}{\langle e_{\mathcal{C}} \rangle_0} + O(\nu^2) \\ &= -2\nu \sum_j \int_0^{\infty} dt \frac{\langle \delta r_j(t) e_{\mathcal{C}}(0) \rangle_0}{\langle e_{\mathcal{C}} \rangle_0} + O(\nu^2). \end{aligned} \quad (24)$$

We define

$$R_{\mathcal{C}} \equiv \frac{1}{\langle e_{\mathcal{C}} \rangle_0} \sum_j \int_0^{\infty} dt \langle \delta r_j(t) e_{\mathcal{C}}(0) \rangle_0 \quad (25)$$

as the propensity [38] for activity R associated with configuration \mathcal{C} : this may be obtained by averaging the observable R over trajectories with initial condition \mathcal{C} . Hence,

the effective potential of configuration \mathcal{C} in the presence of the bias ν is given, to leading order, by its propensity:

$$\Delta V_{\mathcal{C}} = -2\nu R_{\mathcal{C}} + O(\nu^2). \quad (26)$$

Hence, at this order, all effective interactions may be obtained numerically by the relatively simple procedure of calculating propensities. However, this does not address the central challenge associated with characterising the effective interactions. After all, if the system size is N , then the propensity $R_{\mathcal{C}}$ is a set of 2^N numbers: one must still address how the dependence of $R_{\mathcal{C}}$ on the structure of the system can be represented in a useful way. This will be the main strength of the variational approach in Section 6, below.

4.1. Enhancement of the density $\langle n_i \rangle_{\nu}$

In the remainder of this section, we use (22) to investigate the effect of a small bias ν on the structure of the system. We begin with the response of the mean density of up-spins: $\delta \langle n_i \rangle$. We recall from (19) that equilibrium two-time correlation functions vanish unless they involve observables on overlapping regions of the chain, so that

$$\delta \langle n_i \rangle = 2\nu \int_0^{\infty} dt \langle \delta n_i(0) [\delta r_{i+1}(t) + \delta r_i(t)] \rangle_0. \quad (27)$$

The dominant contribution to this response appears because $r_{i+1} > 0$ if and only if $n_i = 1$: physically, this is the statement that if spin i is up then spin $i+1$ is able to flip. The correlation function in the expression for $\delta \langle n_i \rangle$ that corresponds to this effect is

$$\begin{aligned} \langle \delta n_i(0) \delta r_{i+1}(t) \rangle_0 &= \langle \delta n_i(0) [(1-c)n_i(t)n_{i+1}(t) + cn_i(t)\bar{n}_{i+1}(t)] \rangle_0 \\ &\approx 2c(1-c)G_1^0(t), \end{aligned} \quad (28)$$

where the single-site autocorrelation function $G_1(t) = \langle \delta n_i(t') \delta n_i(t' + t) \rangle_{\nu}$ and the superscript 0 indicates that we evaluate it at equilibrium ($\nu = 0$). The approximate equality holds if $\langle n_i(0)n_i(t)n_{i+1}(t) \rangle \approx \langle n_i(0)n_i(t) \rangle \langle n_{i+1}(t) \rangle$, which is to be expected, based on quasiequilibrium arguments along the lines of those in Section 3.2.

The function $G_1^0(t)$ decays from $c(1-c)$ to 0 on the time scale τ_0 . We approximate the time-integral in Eq. 27 by multiplying its maximal value by this relaxation time, leading to $\delta \langle n_i \rangle \simeq 4\nu c^2 \tau_0$, which diverges as $c \rightarrow 0$ (recall that τ_0 diverges faster than any power of $1/c$). Thus, the response of the density ρ to the field ν diverges very quickly as $c \rightarrow 0$. The strong quasiequilibrium correlation between ρ and R means that R also responds very strongly, consistent with the large value of $\chi_R(0)$ shown in Fig. 1.

4.2. Spatial structure in the biased state

Given that the up-spin density $\langle n_i \rangle$ responds strongly to the bias ν already within the linear response regime, the next step is to consider the spatial correlations that accompany this increase.

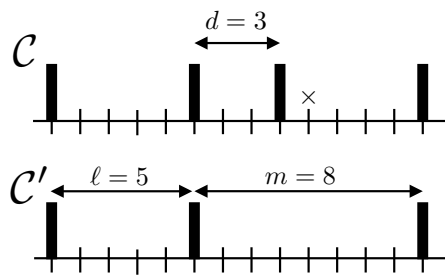


Figure 4. Sketch illustrating the configurations \mathcal{C} and \mathcal{C}' discussed in Section 4.2. Black bars indicate up spins ($n_i = 1$). At low temperatures, the hierarchy of energy scales in the East model means that \mathcal{C} will almost certainly relax to \mathcal{C}' on a time scale τ_3 given by (2); this process is much faster than any other local relaxation mechanism. The propensity $R_{\mathcal{C}}$ differs from $R_{\mathcal{C}'}$ primarily due to the facilitated site that is marked with a \times .

We first consider two configurations \mathcal{C} and \mathcal{C}' , with \mathcal{C} having one more up spin than \mathcal{C}' , as shown in Fig. 4. On increasing ν , we expect the probability of \mathcal{C} to be enhanced with respect to \mathcal{C}' , since the density of up spins is increasing. To obtain the enhancement of \mathcal{C} with respect to \mathcal{C}' , it is sufficient to estimate the propensity difference $R_{\mathcal{C}} - R_{\mathcal{C}'}$. We focus on the domains in the system, defined as in Sec. 3.3 (each up spin starts a new domain, and the domain length is the distance to the next up spin to the right). As in Fig. 4, let the domains in the region of interest of \mathcal{C}' be (\dots, ℓ, m, \dots) and those in \mathcal{C} be $(\dots, \ell, d, m-d, \dots)$. The two configurations coincide exactly in regions indicated by (\dots) .

We further assume that $\alpha_m, \alpha_\ell > \alpha_d$, where the barrier height α_ℓ was defined in (1). Then, the hierarchical relaxation in the East model means that as $c \rightarrow 0$, the local time evolution of \mathcal{C} and \mathcal{C}' is deterministic, in the sense that \mathcal{C} relaxes to \mathcal{C}' , on a time scale τ_d , given by (2). (For small c , the probability that \mathcal{C} relaxes to some other local structure is vanishingly small, due to the separation of time scales in the problem.) After the time lag τ_d , the two configurations behave the same, so all contributions to $R_{\mathcal{C}} - R_{\mathcal{C}'}$ come from times smaller than τ_d . The dominant contribution to $R_{\mathcal{C}} - R_{\mathcal{C}'}$ comes from the spin marked \times in Fig. 4. This spin is facilitated throughout the time τ_d so its contribution to $R_{\mathcal{C}}$ is approximately $2c\tau_d$. (This may be shown using an analysis similar to that leading to (28) above, or the quasi-equilibrium argument explained at the end of Sec. 3.2.) Thus, the enhancement of \mathcal{C} with respect to \mathcal{C}' is determined by

$$\Delta V_{\mathcal{C}'} - \Delta V_{\mathcal{C}} = 2\nu(R_{\mathcal{C}} - R_{\mathcal{C}'}) + O(\nu^2) \approx 4\nu c\tau_d + O(\nu^2), \quad (29)$$

where the approximate equality holds for small c and $2 \leq d \lesssim 1/c$. (For $d = 1$, a similar argument shows that the propensity difference is of order unity: here the dominant contribution comes from the spin at distance $d = 1$ itself, which has a flip rate of $1 - c \approx 1$, rather than its right neighbour.) The key point here is that the difference in effective potential in (29) depends very strongly on the position of the extra up spin in \mathcal{C}' . If $d = 1$ and the extra up spin is adjacent to an existing one, the difference in effective potential between \mathcal{C} and \mathcal{C}' is $\nu \cdot O(1)$, which is small on the natural scale

of ν . But if (for example) $d = 1 + 2^b$ then the enhancement diverges as $\nu \cdot O(c^{-b})$: configurations where the extra up spin is far from any existing spin are very strongly enhanced if $b > 1$.

This strong dependence of ΔV_C on the relative positions of the up spins in \mathcal{C} is the mechanism for the repulsive correlations in $C(x)$ shown in Fig. 2. Configurations where the spins are spaced out have large propensities for activity R , since the up spins increase activity, and widely-spaced up spins persist for longer time within the system. Hence, the effect of the bias ν is to favour configurations \mathcal{C} with long-lived active regions, since these give the largest contributions to R_C .

4.3. Response of $p(d)$ to the bias ν

To further elucidate this effect, we show how ν affects the domain structure in the system, by calculating the response of $p(d)$ at leading order in ν . Recall that $p(d)$ can be written as in Eq. (18) above, in terms of the observable $D_{i,i+r}$ defined in (17). The linear response relation (21) then gives for the enhancement of $p(d)$ at first order in ν

$$\frac{p(d)}{p^0(d)} = 1 + 2\nu \left\langle \left(\frac{n_i D_{i+1,i+d-1} n_{i+d}}{\langle n_i D_{i+1,i+d-1} n_{i+d} \rangle_0} - \frac{n_i}{\langle n_i \rangle_0} \right) \delta R \right\rangle_0 + O(\nu^2) \quad (30)$$

The right hand side of (30) is straightforward to evaluate numerically: see Fig. 2(c).

For small c , the right hand side of (30) may be estimated following the discussion of Sec. 4.1. The first term in the average in (30) has contributions of the form

$$\frac{1}{\langle n_i D_{i+1,i+d-1} n_{i+d} \rangle_0} \int dt \langle [n_i(t') D_{i+1,i+d-1}(t') n_{i+d}(t')] \delta r_j(t) \rangle_0, \quad (31)$$

for which the largest contributions come from $j = i + 1$ and $j = i + d + 1$: these sites are adjacent to the spins that are up at time $t' = t_{\text{obs}}/2$ and hence facilitated. If $j = i + 1$, Eq. (31) gives $\approx 2c\tau_0$ as in Sec. 4.1; the amplitude $2c$ comes from the quasiequilibration rule discussed in Sec. 3.2. However, there is an analogous contribution from the $\langle n_i \delta R \rangle_0$ term in (30) which exactly cancels this effect. Evaluating (31) when $j = i + d + 1$, one obtains $\approx 2c\tau_d$, which is an alternative derivation of the enhancement considered in Sec. 4.2. In addition, there are contributions to (30) of the form of (31), with sites j between i and $i + d$. These spins are down and unfacilitated at time $t = 0$, and the typical time scale for spin $i + a$ to become facilitated is τ_a . Such a spin therefore contributes $-\tau_a \langle r \rangle = -2c^2\tau_a$ to (30). This contribution is smaller than the contribution of site $i + d + 1$, but if d is large then there are many down spins between i and $i + d$, and these contributions become significant. If we use the coarse (over-)estimate $\tau_a \approx \tau_d$, the total contribution from down-spins is $-2(d - 1)c^2\tau_d \approx (-cd)(2c\tau_d)$. Since $\tau_d \approx (cd)\tau_0$, this negative contribution scales with d^2 and thus dominates for large d over the positive contribution from the up-spin at $j = i + d + 1$, $2c\tau_d$, which scales linearly with d . A more refined estimate accounting for the a -dependence of the contributions from the internal down-spins at $i + a$ only changes the prefactor of the leading d^2 -dependence of the negative linear response contribution.

Combining all these results, and taking $c \rightarrow 0$, we expect

$$\frac{p(d)}{p^0(d)} \simeq 1 + A_d \nu / c^{\alpha_d - 1} + O(\nu^2), \quad 2 \leq d \lesssim 1/c; \quad (32)$$

For domains of size 1, one has (by arguments analogous to those in Sec. 4.2)

$$\frac{p(d=1)}{p^0(d=1)} \simeq 1 + A_1 \nu + O(\nu^2), \quad (33)$$

and for large domains

$$\begin{aligned} \frac{p(d)}{p^0(d)} &\simeq 1 + 4\nu(1 - cd)c\tau_d + O(\nu^2) \\ &\simeq 1 - A_d \nu \tau_0 c^2 d(cd - 1) + O(\nu^2), \quad d \gtrsim 1/c. \end{aligned} \quad (34)$$

Here, all the $A_d = O(1)$ as $c \rightarrow 0$.

We observe that for large domain sizes $d \gg 1/c$, the linear response result diverges with d , so the result is necessarily applicable only in a range of ν that becomes vanishingly small as $d \rightarrow \infty$. However, such large domains are extremely rare in any case and the effect of $\nu > 0$ is to *suppress* them very strongly (recall Fig. 2). In this case, the breakdown of perturbation theory in the calculation of $p(d)$ does not lead to any apparent non-perturbative effect in observables like $r(\nu)$ or $C(x)$. On the other hand, if we bias to lower than average activity by taking $\nu < 0$, large domains are *enhanced* non-perturbatively as $d \rightarrow \infty$: this effect drives the phase transition into the inactive state [10], with large domains predominating for all $\nu < 0$.

5. Hierarchy of responses at small c , and link to aging

The results of Section 4 can be summarised by (32-34), which encode a hierarchy of responses to the bias ν . When c is small, the linear responses for different d scale as $\nu/c^{\alpha_d - 1}$. Estimating the range over which this linear response prediction is valid is not a trivial task, because the responses are divergent for large d , consistent with the phase transition to an inactive state as ν becomes negative. However, based on the numerical results of Sec. 3 and the linear response calculation, we can formulate a picture that captures the main features of the responses to the bias, both linear and nonlinear.

The main idea is a generalisation of the quasiequilibrium relation discussed in Section 3.2. That argument indicates that $p(d=1) \approx c$ as long as $\nu \ll 1$, regardless of whether ν is small compared with other powers of c . Put another way, nonlinear responses in (33) do not set in until $\nu \simeq 1$. We are proposing here that similar quasiequilibrium conditions hold for larger d , and small c . In particular, for $\nu/c^{b-1} \ll 1$, domains of sizes $1 \leq d \leq 2^b$ are weakly affected by the bias, so that $p(d) = O(c)$ as $c \rightarrow 0$. This corresponds to the assumption that the linear response prediction (32) remains accurate until the relative linear response correction becomes of order unity. [More precisely, we expect that nonlinear corrections to $p(d)$ are at most of absolute size $O(c)$ in this regime, not $O(1)$.] On the other hand, the perturbative expansion indicates that larger domains ($d > 2^b$) have much larger responses which must be nonlinear in

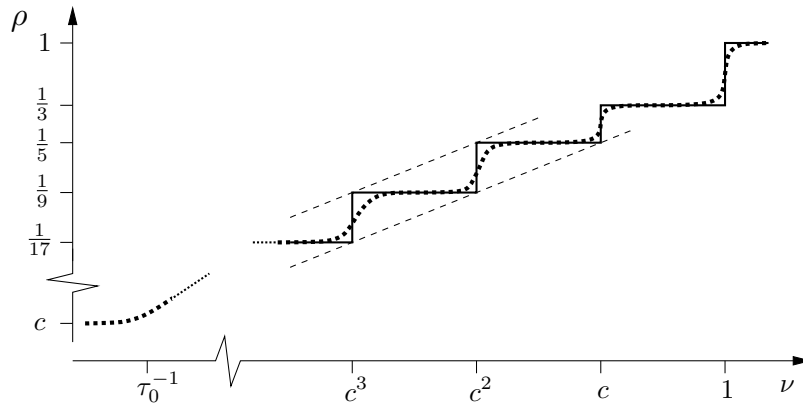


Figure 5. Sketch showing how the density of up spins $\rho = \langle n_i \rangle_\nu$ depends on ν , for very small c . Both axes are logarithmic. The solid line shows the limiting behaviour as $c \rightarrow 0$, taken at fixed $(\ln \nu)/(\ln c)$, while the dashed line shows the expected behaviour for a system with small positive c . The effect of the bias ν becomes significant when $\nu \approx \tau_0^{-1}$, the inverse bulk relaxation time. As ν is increased further towards unity, the system eventually responds in a sequence of steps. We expect a weak dependence on ν whenever $c^b \ll \nu \ll c^{b-1}$ for integer b , leading to plateaus in ρ . Within each plateau ($b \geq 1$), our conjecture is that the spacing between up spins converges to $1 + 2^b$ as $c \rightarrow 0$, so $\rho \rightarrow \frac{1}{1+2^b}$. For large b , the plateaux are then bounded by $\rho = 2^{-b-1}$ and $\rho = 2^b$, corresponding to power-law behaviour $\rho \sim 2^{-(\ln \nu)/(\ln c)} \sim \nu^{T \ln 2}$ (dashed lines). From the quasiequilibrium argument, one expects also $r(\nu) \approx 2c \langle n_i \rangle_\nu = 2c\rho(\nu)$: when comparing this prediction with Fig. 1, we emphasise that those numerical results are still rather far from the small- c limit.

nature: we expect that $p(d)$ has a non-zero limit for those domain sizes, so that the mean domain size (and hence $r(\nu)$ and $\langle \rho \rangle_\nu$) remain finite as $c \rightarrow 0$.

To illustrate this effect, recall Fig. 3 which shows data for $\nu = c^2$, as c is decreased. One sees that $p(d)$ for $d \leq 4$ decreases as c is reduced, consistent with the expectation that it tends to zero as $c \rightarrow 0$; on the other hand $p(d)$ has a non-zero limit for $d \geq 5$. We identify an emergent length scale $d^* = 5$: domains smaller than d^* have a vanishing probability in the relevant limit, domains of size close to d^* are very likely, while larger domains have finite (typically smaller) probabilities. In general, if $\nu = c^b$ for some integer b , and we consider the limit $c \rightarrow 0$, then one expects a similar situation with a length scale $d^* = 1 + 2^b$.

It is also useful to consider the case $c^b \ll \nu \ll c^{b-1}$ with $c \rightarrow 0$. Then, one expects small domains ($d \leq 2^b$) to be quasi-equilibrated with $p(d) \simeq c$, while larger domains ($d > 2^b$) should have $p(d) = O(1)$, weakly dependent on ν . In fact, our numerical results indicate that almost all domains will be of size $d = 1 + 2^b$ in this limit, leading to a finite density of up spins $\langle n_i \rangle_\nu = 1/(1+2^b)$. This allows the system to maximise the escape rate r , subject to the quasiequilibrium constraint on smaller domains. The simplest case is the limit $c \ll \nu \ll 1$ where this analysis predicts $\langle n_i \rangle_\nu \approx \frac{1}{3}$. This behaviour is consistent with Fig. 1(c), where $\rho(\nu) = \langle n_i \rangle_\nu$ increases quickly to a value close to $\frac{1}{3}$ at $\nu \approx c = 0.1$ before increasing more weakly for large ν . The value of c is not small enough to saturate

the limit and establish a clear plateau in $r(\nu)$ but the numerical results are certainly consistent with the picture proposed here. Returning to the general argument, Fig. 5 summarizes the predicted hierarchy of responses in a sketch. The plateau structure in $\rho(\nu)$ and its power-law asymptote $\rho \sim \nu^{T \ln 2}$ are intriguingly similar to the one observed in the out-of-equilibrium aging dynamics of the East model [26], with ν playing the role of the inverse age. A similar generalisation of quasiequilibrium to that described here can also be observed in equilibrium dynamics, through an analysis of metastable states [39].

6. Variational approaches

To investigate the response of the system to ν beyond first order, we exploit a variational method, which relies on the time-reversal symmetry of the ν -ensemble. The master operators $\mathbb{W}_K(s)$ and $\mathbb{W}_R(\nu)$ may be symmetrised, as described in Sec. 2.2. Hence (see Appendix A.1 and Refs. [10, 18]), one may obtain the effective potential $\Delta V_{\mathcal{C}}$ by minimising the variational ‘free energy’ (per site):

$$F(\Delta \tilde{V}) = -N^{-1} \frac{\sum_{\mathcal{C}, \mathcal{C}'} e^{-\Delta \tilde{V}_{\mathcal{C}'}/2} [\mathbb{W}_R(\nu)]_{\mathcal{C}', \mathcal{C}} e^{-\Delta \tilde{V}_{\mathcal{C}}/2} p_{\mathcal{C}}^0}{\sum_{\mathcal{C}} e^{-\Delta \tilde{V}_{\mathcal{C}}} p_{\mathcal{C}}^0}, \quad (35)$$

where $\Delta \tilde{V}$ is a variational estimate of the effective potential, $[\mathbb{W}_R(\nu)]_{\mathcal{C}', \mathcal{C}}$ is a matrix element of the operator $\mathbb{W}_R(\nu)$, and $p_{\mathcal{C}}^0 = e^{-\beta \sum_i n_i} / (1 + e^{-\beta})^N$ is the equilibrium probability of configuration \mathcal{C} . On minimising $F(\Delta \tilde{V})$ over all the $\Delta \tilde{V}_{\mathcal{C}}$, the minimal value of F is equal to the dynamical free energy $\psi_R(\nu)$, and $\Delta \tilde{V}_{\mathcal{C}}$ is equal to the effective potential $\Delta V_{\mathcal{C}}$. Hence, if a suitable exact parameterisation of $\Delta \tilde{V}_{\mathcal{C}}$ may be found, one may obtain the effective potential by minimising $F(\Delta \tilde{V})$. More typically, one makes an approximate parameterisation of the effective potential, and minimises F with respect to the variational parameters. For a given parameterisation of $\Delta \tilde{V}_{\mathcal{C}}$ (“trial potential”), we denote the minimal value of F by F^{var} and the corresponding estimate of $\Delta \tilde{V}_{\mathcal{C}}$ by $\Delta V_{\mathcal{C}}^{\text{var}}$.

We note in passing that an alternative to this variational approach would be to use a density-matrix renormalisation group method (see e.g. [40]), which is related to a variational search over matrix product states [41]. However, the advantage of (35) is that it has a clear interpretation as a variational search in a given space of effective potentials ΔV .

6.1. Trial potential functions

We first describe three trial potentials that we have investigated.

6.1.1. Block model. A completely general trial potential should include all possible m -body interactions of all ranges. To approximate this, we consider interactions within ‘blocks’ of size B . The potential includes m -body interactions up to $m = B$, with a maximal interaction range of $B - 1$. It also permits a transfer-matrix representation

of the probability distribution over configurations \mathcal{C} in the ν -ensemble. The idea is to consider a block of spins, $\mathcal{B}_i = (n_i, n_{i+1}, \dots, n_{i+B-1})$, and that each possible block configuration has its own contribution to the trial potential. That is, if $e_{\mathcal{B}}(\mathcal{B}_i)$ is an indicator function, equal to unity when block \mathcal{B}_i has the specific configuration \mathcal{B} and zero otherwise, then $\Delta\tilde{V}_{\mathcal{C}} = \sum_i \sum_{\mathcal{B}} z_{\mathcal{B}} e_{\mathcal{B}}(\mathcal{B}_i)$, where the $z_{\mathcal{B}}$ are variational parameters that determine the block probabilities.

There are 2^B trial weights $z_{\mathcal{B}}$, but these in fact provide an overcomplete basis for the possible interactions in $\Delta\tilde{V}$, because the numbers of blocks in the 2^B different states are not independent. For example, if $N_{010} = \sum_i \bar{n}_i n_{i+1} \bar{n}_{i+2}$ is the number of blocks with configuration ‘010’ (and similarly for other block configurations) then one may use $\bar{n} = 1 - n$ to write $N_{010} = \sum_i [n_{i+1} \bar{n}_{i+2} - n_i n_{i+1} \bar{n}_{i+2}] = \sum_i [n_{i+1} \bar{n}_{i+2} n_{i+3} + n_{i+1} \bar{n}_{i+2} \bar{n}_{i+3} - n_i n_{i+1} \bar{n}_{i+2}] = N_{101} + N_{100} - N_{110}$. Here the last equality involved a relabelling within the summation, which relies on the periodic boundaries of the system. In this way, the numbers of all blocks of length B that begin with a down spin (‘0’) can be expressed exactly in terms of numbers of blocks that begin with an up spin (‘1’). There are 2^{B-1} such numbers, and it is then not difficult to see that one can equivalently specify the numbers of all blocks of length 1 to B that start *and* end with a 1. (E.g. for $B = 2$ one can use $N_1 = N_{11} + N_{10}$ and N_{11} instead of N_{10} and N_{11} .) Using this latter representation, a general trial potential for the block model with block length $B = 2$ can be written as

$$\Delta\tilde{V}_{\mathcal{C}} = \sum_i h n_i + J n_i n_{i+1}, \quad (36)$$

which includes a field h and a two-body Ising-like coupling as variational parameters. For higher B one has in addition all interaction terms up to range $B - 1$ and involving up to B spins.

In Appendix A.1, we show how the variational free energy in (35) may be calculated for this model, given the weights $z_{\mathcal{B}}$. The method relies on a transfer matrix representation of $e^{-\Delta\tilde{V}_{\mathcal{C}}}$. This allows F to be minimised (numerically) over the $z_{\mathcal{B}}$, leading to an estimate $\Delta\tilde{V}^{\text{var}}$ for the effective interactions.

6.1.2. p_d model. The block model is a general variational ansatz, but the number of variational parameters increases exponentially with the maximal interaction range $B - 1$. In the following, this will limit our numerical results to $B \leq 6$. As we have already discussed, Fig. 2 indicates that the true effective potential $\Delta V_{\mathcal{C}}$ includes rather long-ranged interactions, which would require much larger values of B to capture them.

For this reason, we have designed trial potentials in order to account for the particular structures that occur in the East model. Instead of including all interactions up to range B , these potentials include a specific subset of long-ranged interactions. In particular, we concentrate on the ‘domains’ discussed above and construct a $\Delta\tilde{V}_{\mathcal{C}}$ that depends only on the sizes of these domains. Thus, this trial potential will be accurate if all information about structure in the ν -ensemble is contained in the distribution $p(d)$

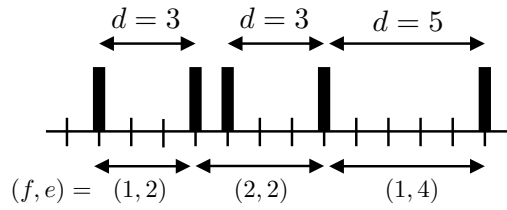


Figure 6. Sketch showing how the domains are identified in the p_{fe} and p_d models. The (unlabelled) domain of size $d = 1$ in the p_d representation is combined with the adjacent domain to form an composite domain with $(f, e) = (2, 2)$ in the p_{fe} model.

shown in Fig. 2. Formally, we include specific m -body interactions of all ranges

$$\Delta \tilde{V}_C = \sum_{i,d} z_d n_i D_{i+1,i+d-1} n_{i+d}, \quad (37)$$

where the z_d are variational parameters associated with the possible domain sizes. Given these weight factors, one may derive the distribution of domain sizes $p(d)$ associated with this variational ansatz. In fact, it is convenient to work directly with this distribution, which we denote by p_d to distinguish its status as a variational parameter from a measured $p(d)$.

The variational free energy is

$$F_d = \frac{1}{\sum_d d p_d} \left\{ (1 - \nu) [c + (1 - 2c)p_1] - 2\sqrt{c(1 - c)} \sum_{d \geq 2} \sqrt{p_1 p_{d-1} p_d} \right\}. \quad (38)$$

The derivation of this free energy is discussed in Appendix A.3: it is to be minimised subject to the normalisation constraint $\sum p_d = 1$.

In principle the sums over d in (38) run over all $d \geq 1$ and $d \geq 2$ respectively, but for numerical work we truncate the sums at a cutoff d^* by assuming $p_d = 0$ for $d > d^*$: domains much larger than $1/c$ are extremely rare in the system so the results depend negligibly on d^* .

6.1.3. p_{fe} model. The p_d model gives useful results, but we will find that it does not account accurately for the quasiequilibrium conditions described in Sec. 5. This shortcoming limits its accuracy, so we discuss one systematic improvement to the p_d model, which captures some features of this quasiequilibration.

Recall that in the p_d model, the system is divided into domains that start at each up spin, and each domain is assumed to be independent. Each domain then consists of a single up spin, followed by a block of $d - 1$ down spins. An alternative and more general assumption is to start domains at each occurrence of the block ‘01’. The situation is illustrated in Fig. 6. Each domain consists of a block of up spins, followed by a block of down spins. The domain state is specified by 2 numbers f, e , so that there are f (“full”) up spins and e (“empty”) down spins. Fig. 6 shows that the domains in this ‘ fe ’-representation are in general larger than those in the p_d -model representation. We then

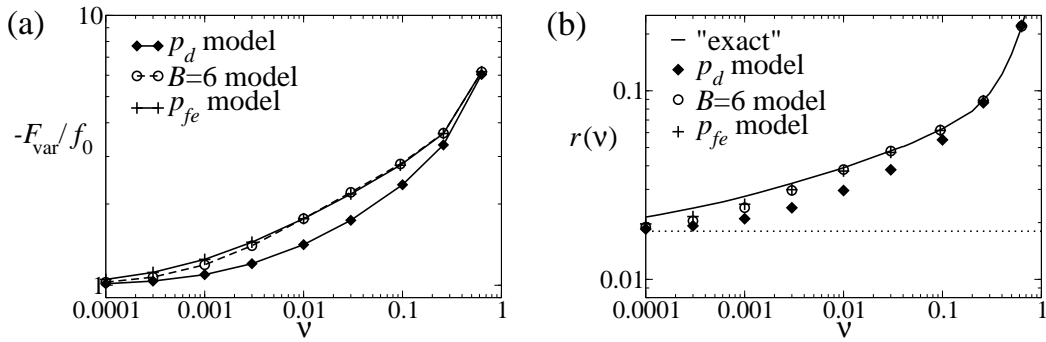


Figure 7. (a) Variational free energy, F^{var} at $c = 0.1$, using different trial potentials. Since F^{var} varies over several orders of magnitude, we plot $-F^{\text{var}}/f_0$, where $f_0 = \nu r(0)$. One has $-F^{\text{var}}/f_0 \rightarrow 1$ as $\nu \rightarrow 0$, so that $F^{\text{var}} = -f_0 + O(\nu^2)$ at small bias. A larger number in this representation indicates a better trial potential: the p_{fe} model and the $B = 6$ block model perform significantly better than the (simpler) p_d model. (b) Variational estimates of $r(\nu)$ compared with the numerical results shown in Fig. 1 (labelled “exact”). The dotted (horizontal) line indicates $r(0) = 2c^2(1 - c)$.

construct an effective potential on the assumption that the fe -domains are independent:

$$\Delta \tilde{V}_C = \sum_{i,f,e} z_{fe} \bar{n}_{i-1} \cdot U_{i,i+f-1} \cdot D_{i+f,i+f+e-1} \cdot n_{i+f+e}, \quad (39)$$

where the z_{fe} are the variational parameters. We refer to this model as the ‘ p_{fe} model’. As with the p_d model, it is more convenient to work with the probability distribution over the domains, which we denote by p_{fe} . One can show that the p_d model corresponds to the special case $p_{fe} = p_1^{f-1} p_{e+1}$, which emphasises that the p_{fe} model is a generalisation of the p_d model. In particular, the p_{fe} model allows the length e of a down-block to depend on the number of adjacent up spins to its left.

The derivation of the variational free energy for the p_{fe} model is discussed in Appendix A.4: the result is

$$F_{fe} = \frac{1}{\sum_{fe} (f+e) p_{fe}} \cdot \left\{ (1-\nu) \sum_{fe} p_{fe} [c + (f-1)(1-c)] - 2\sqrt{c(1-c)} \left[\sum_{fe} \sqrt{p_{f,e+1} p_{f+1,e}} + \sum_{f,f',e} \sqrt{p_{f'1} p_{fe} p_{f+f'+1,e}} \right] \right\}, \quad (40)$$

The minimisation is subject to the normalisation constraint $\sum_{f,e} p_{fe} = 1$. Numerically we again model p_{fe} explicitly only up to cutoffs f^* and e^* . These cutoffs cannot be made too large because the number of variational parameters is now $f^* e^*$. To soften the impact of the cutoffs we therefore do not set p_{fe} directly to zero beyond the cutoffs, but assume an exponential tail instead that is obtained by linear extrapolation of $\ln p_{fe}$.

6.2. Variational results

We have used numerical minimisation to obtain results for the three trial potentials, at $c = 0.1$. Fig. 7 shows the values of F^{var} that we obtained, and the corresponding

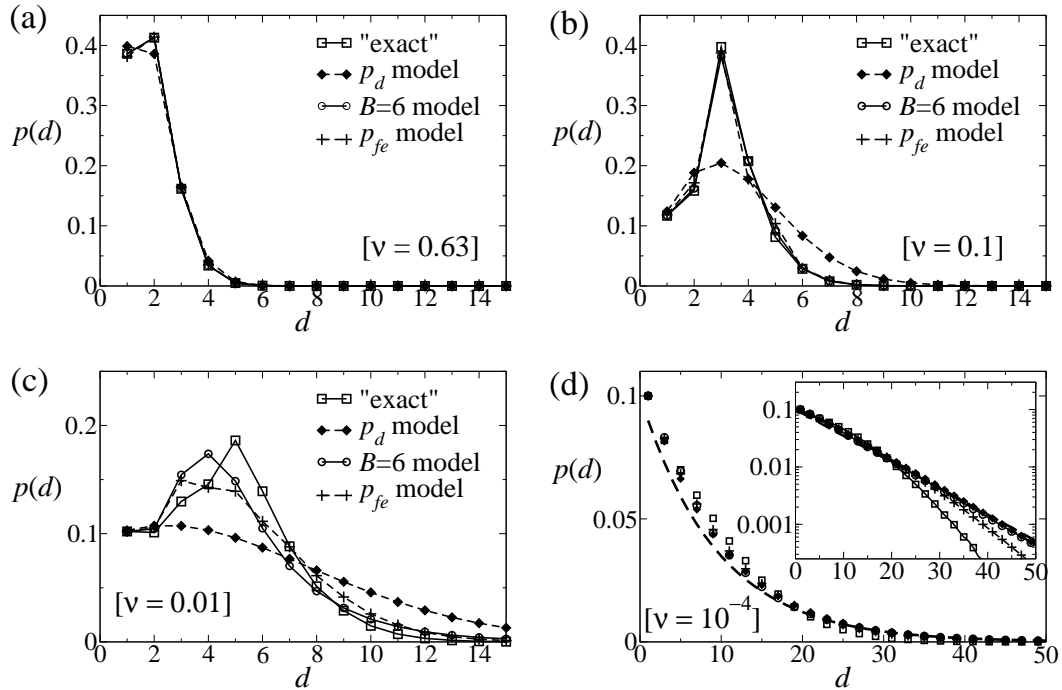


Figure 8. (a-d) Comparison between the domain-size distributions $p(d)$ obtained numerically by TPS or exact diagonalisation (labelled “exact”) with those obtained from (approximate) variational analyses. All results are at $c = 0.1$, and for four different values of ν as shown in each plot. The variational approaches are most effective for larger ν when domains are typically short. In panel (d), the unbiased distribution $p^0(d)$ is shown as a dashed line. The inset shows the same results on a logarithmic scale, emphasising the differences in the tails of the distribution. For this value of ν , the p_d model and the $B = 6$ model give similar results, and are both close to the unbiased distribution $p^0(d)$. (The legend is omitted: symbols are the same as in all other panels.)

estimates for $r(\nu)$. These are compared with the numerical results shown in Fig. 1. In general, the p_{fe} model and the $B = 6$ block model seem to capture the data quite well, while the p_d model gives less good agreement. It is also clear from $r(\nu)$ that the variational models perform best for larger ν , with significant deviations for smaller ν .

Since the minimisation yields the effective interaction potential ΔV_C^{var} , we are also able to calculate variational predictions for one-time quantities in the ν -ensemble. As a stringent test of these variational distributions, Fig. 8 shows the estimates for $p(d)$ that we obtain from the variational treatment, compared with numerical results from Sec. 3. For the largest ν ($= 0.63$), all three models describe the data quite accurately, although deviations are apparent for the p_d model. Nearly all domains in this system are short, so one can expect a relatively simple effective interaction to accurately describe these data.

For $\nu = 0.1$, there is clear structure in the system, including a most probable domain size of $d = 3$, which is captured quite accurately by both the p_{fe} model and the $B = 6$ block model, although not by the p_d model. We recall from Sec. 4 that for

$\nu \approx c$, one expects domains of lengths $d \leq 2$ to have probabilities of order c , while larger domains have probabilities of order unity. This is consistent with the most likely domain size of $d = 3$.

For smaller ν , the structure in $p(d)$ becomes more complex, and even the p_{fe} and $B = 6$ models fail to accurately describe the effective interactions in the system. We note in particular that $\nu = 0.01$ corresponds to $\nu = c^2$ for this case, in which case Sec. 4 predicts that $p(d)$ should be of order unity for $d \geq 5$, but of order c for $d \leq 4$. It is apparent that the p_{fe} and $B = 6$ models fail to capture this aspect of the linear response to the system. Finally, we note that for very small $\nu \approx 10^{-4}$, these variational models significantly underestimate the suppression of large domains. For the block model, it is easily shown (see Appendix A.2) that $p(d)$ must decay exponentially for $d > B$, in contrast to the faster decrease found in our numerically exact results.

It is clear from the numerical results in Figs. 7 and 8 that the p_d model gives quite a crude description of the effective interactions in the system. However, this model can be studied analytically, with several useful results, which we summarize briefly to conclude this section. Looking at the linear response for small ν , one finds for p_1 a positive relative correction of $O(\nu)$ in line with the notion of quasi-equilibrium for small ν , while for all other p_d the relative correction is $O(\nu/c)$. With increasing d the correction becomes negative and its amplitude grows, so that the model captures at least qualitatively the large- d divergence of the perturbative correction shown in Fig. 2(c). For nonzero ν one can show that p_d must decay faster than exponentially, indicating the presence of long-ranged effective interactions that will make block models with fixed block lengths poor approximations. Finally one can look at the $c \rightarrow 0$ limit of the p_d model at fixed small (but non-zero) ν . One finds $p_1 = O(c)$, consistent again with quasi-equilibrium, while $p_d = O(1)$ for $d \geq 2$. The predicted activity is $r(\nu) = c \cdot f_r(\nu)$ with f_r of $O(1)$. Assuming that quasiequilibrium along the lines of (20) holds, one infers that $\langle \rho \rangle_\nu = f_\rho(\nu)$ with $f_\rho(\nu) \approx \frac{1}{2} f_r(\nu)$ of $O(1)$: the density of up-spins remains finite, in contrast to the equilibrium case $\nu = 0$ where $\langle \rho \rangle_0 = c$ vanishes as $c \rightarrow 0$. From the discussion of Sec. 5, one would expect that $f_\rho(\nu \rightarrow 0) = 1/3$, so $f_r(\nu \rightarrow 0) = 2/3$. The p_d model predicts correctly that f_r and f_ρ are of order unity as $c \rightarrow 0$, but gives a rather poor estimate of the shapes of the function, yielding e.g. $f_r(\nu) \sim \nu^{1/2}$ for small ν .

6.3. Limitations of variational schemes: the complex hierarchical response to ν

The results of Sec. 4 suggest a hierarchy of responses to the bias ν , as discussed in Sec. 5. The general idea is that the system remains quasiequilibrated on short length scales, while large length scales respond strongly to the bias. The linear response of a configuration to the bias is given by its propensity for activity, $R_{\mathcal{C}}$. We find that $R_{\mathcal{C}}$ is dominated by long time scales in the model, which are typically associated with large scale structures in the configuration \mathcal{C} .

Fig. 8 shows data at $\nu = 10^{-4}$ and $c = 0.1$ which indicate that none of the variational models used here are successful in capturing the long-ranged correlations that appear

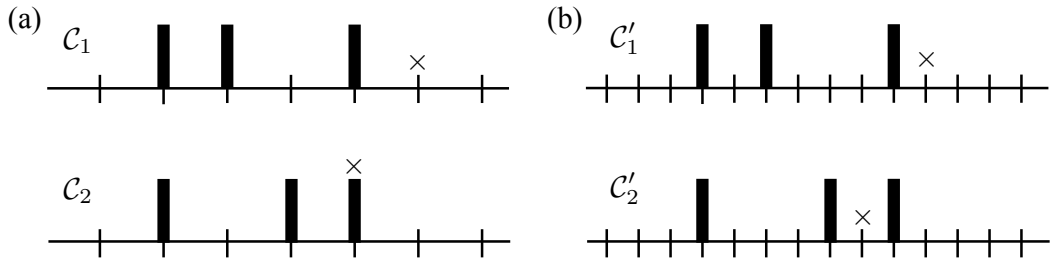


Figure 9. (a) Configurations \mathcal{C}_1 and \mathcal{C}_2 that illustrate how the propensity depends on correlations between domains, and not just on their domain lengths. (See discussion in main text.) Vertical bars indicate up spins ($n_i = 1$) as before. The \times signs mark the sites whose contributions are most relevant when comparing the propensities of these configurations. (b) Configurations \mathcal{C}'_1 and \mathcal{C}'_2 indicate that while some relevant correlations between domains can be captured within the p_{fe} model, there are still configurations that have different propensities, but equal probabilities within the p_{fe} model.

in this perturbative regime. While the $B = 6$ block model necessarily excludes long-ranged correlations, the failure of the p_{fe} model indicates that domain sizes alone are not sufficient to predict the propensities $R_{\mathcal{C}}$, so that $\Delta\tilde{V}$ necessarily includes interactions between domains of different sizes.

To see how structure among domains is important in determining their propensities (and hence their effective potentials), it is useful to consider the configurations \mathcal{C}_1 and \mathcal{C}_2 shown in Fig. 9(a). Within the p_d model, these configurations are equally likely. However, to estimate their propensities, one follows the analysis of Sec. 4.2 and first assumes that the least long-lived up spin in each state relaxes quickly to 0. Then one considers the contributions to $R_{\mathcal{C}_1}$ and $R_{\mathcal{C}_2}$ from the spins marked \times . In \mathcal{C}_1 , the relevant spin remains facilitated for an $O(c^{-2})$ time scale while in \mathcal{C}_2 it remains facilitated for an $O(c^{-1})$ time scale. The contributions to $R_{\mathcal{C}_1}$ and $R_{\mathcal{C}_2}$ are therefore $O(1/c)$ and $O(1)$ respectively: the enhancement of \mathcal{C}_1 in the presence of the bias is much stronger than that of \mathcal{C}_2 . The p_d model cannot capture this difference. However, within the p_{fe} model, configurations \mathcal{C}_1 and \mathcal{C}_2 have independent weights, proportional to $p_{2,1}p_{1,e}$ and $p_{1,1}p_{2,e}$ respectively. Thus, the model accounts for their different enhancements in the presence of the bias. The argument that facilitated spins remain quasiequilibrated implies that $p_{f+1,e} \approx cp_{f,e+1}$, so (for example) $p_{2,1} \approx cp_{1,2}$. The numerical results obtained from the p_{fe} model are broadly consistent with this result. This effect may be also rationalised in the superspin picture of Ref. [26] if one removes facilitated up spins to leave (relatively) long-lived superspins. It is the spacing of the superspins that determines the propensity.

While the p_{fe} model performs better than the p_d model for configurations \mathcal{C}_1 and \mathcal{C}_2 , its main shortcoming may be understood in a similar way. One generalises the previous argument by multiplying all length scales by two and all time scales by $1/c$. The configurations \mathcal{C}'_1 and \mathcal{C}'_2 shown in Fig. 9(b) have equal probability within the p_{fe} model but the spin marked with \times in \mathcal{C}'_1 remains facilitated for a time that is $O(c)$ shorter than the marked spin in \mathcal{C}'_2 . Thus, the relative propensities of the configurations

are different, but this effect is missed within the p_{fe} model. Thus, the p_{fe} model can distinguish configurations that respond to the bias at $O(\nu)$ from those that respond at $O(\nu/c)$, but it cannot distinguish those that respond at $O(\nu/c^2)$ or greater.

A perfect trial potential would distinguish configurations that respond at $O(\nu/c^b)$, for all the possible values of b discussed in Sec. 5. However, the point here is that the p_{fe} model specifically allows for p_d -domains with $d = 1$ to be correlated with other domains to their right. All other correlations amongst domains are forbidden. But to resolve the difference in propensity between \mathcal{C}'_1 and \mathcal{C}'_2 in Fig. 9, one requires specific correlations between domains with $d = 2$ and other domains. And while including such correlations explicitly would allow characterisation of configurations which respond at $O(\nu/c^2)$, the procedure used to derive \mathcal{C}'_1 and \mathcal{C}'_2 from \mathcal{C}_1 and \mathcal{C}_2 can be repeated to obtain a \mathcal{C}''_1 and \mathcal{C}''_2 , one of which will respond at $O(\nu/c^3)$. Making this distinction will rely on specific correlations among domains with $d = 4$ and greater. One sees that accounting specifically for these increasingly complex correlations quickly becomes prohibitive. The p_{fe} -model serves as a useful indication of the physics at work and the kinds of effective interaction that are expected. We are exploring further improvements to this trial potential, but these are beyond the scope of this study.

7. Outlook

To end this article, we discuss which of the features of the analysis here may be generalised to other glassy systems in the presence of biased activity. At the perturbative level, we showed that the response of a configuration depends only on its propensity: this result is general. The problem of finding the effective interactions for the linear response regime is therefore equivalent to finding a model that accurately describes the propensity of a configuration. In the East model, this requires consideration of structure on quite large length scales, and an accurate description requires identification of the long-lived superspins in the system, which is a difficult task. In the general case, we have shown that variational calculations can be useful in showing what effective interactions can reproduce the correlations found in biased states. However, the trial distributions must be informed by considerable physical insight to yield useful results.

On the other hand, the hierarchy of time scales and the quasi-equilibrium features of the biased East model do simplify the description of the effective interactions. If the model is quasiequilibrated on short length scales, this means that effective interactions on those scales are weak and may be neglected. Recent work on atomistic model glass-formers [21] and spin-glass models [12] does indicate that time-scale separation in biased ensembles can be used to simplify the description of the biased states. This may well be a useful simplification to guide future studies.

Acknowledgments

We thank Fred van Wijland and Juan P. Garrahan for many useful discussions on large deviations, and emergent structure in ensembles of trajectories. RLJ was supported by the EPSRC through grant EP/I003797/1.

Appendix A. Calculations using variational trial potentials

Appendix A.1. Block model

In this section, we describe how the variational free energy in (35) is calculated for the block model of Sec. 6.1.1. The block configuration $\mathcal{B}_i = (n_i, n_{i+1}, \dots, n_{i+B-1})$ is a binary string of length B , and a configuration may be specified by its block configurations: $\mathcal{C} = (\dots, \mathcal{B}_i, \mathcal{B}_{i+1}, \dots)$. The blocks are overlapping, so the specification is overcomplete: the final $B - 1$ spins in \mathcal{B}_i are equal to the first $B - 1$ spins in \mathcal{B}_{i+1} , etc.

We write $\tilde{p}(\mathcal{C}) = e^{-\Delta\tilde{V}_{\mathcal{C}} - \beta E_0(\mathcal{C})}$ where $E_0 = \sum_i n_i$ is the energy of the East model, and we identify \tilde{p} as the (unnormalised) trial probability distribution associated with the trial potential $\Delta\tilde{V}$. From (36), one has $e^{-\Delta\tilde{V}_{\mathcal{C}}} = \prod_i e^{-z_{\mathcal{B}_i}}$. It is convenient to write $\tilde{p} = \prod_i M_{\mathcal{B}_i, \mathcal{B}_{i+1}}$, where $M_{\mathcal{B}_i, \mathcal{B}_{i+1}} = e^{-z_{\mathcal{B}_i} - \beta n_i}$, recalling that the last $B - 1$ spins of \mathcal{B}_i always coincide with the first $B - 1$ spins of \mathcal{B}_{i+1} . One then generalises M to a “transfer matrix” of size $2^B \times 2^B$, by setting $M_{\mathcal{B}, \mathcal{B}'} = 0$ if the last $B - 1$ spins of \mathcal{B} do not coincide with the first $B - 1$ spins of \mathcal{B}' . With this choice, averages with respect to \tilde{p} can be evaluated as matrix traces. E.g., for a periodic chain of length L , one has $\sum_{\mathcal{C}} \tilde{p}(\mathcal{C}) = \text{tr}(M^L)$. We note that for $B = 2$, the block model reduces to the 1d Ising model, which would usually be solved using a 2×2 transfer matrix: the method presented here uses a 4×4 transfer matrix. This is less efficient numerically, but its generalisation to larger B is simpler.

We now relate the matrix M to the variational free energy F defined in (35). To this end, we symmetrise the operator in (35), noting that $[\mathbb{W}_R(\nu)]_{\mathcal{C}', \mathcal{C}} p^0(\mathcal{C}) = \sqrt{p^0(\mathcal{C}')} [\sum_i \hat{H}_i(\nu)]_{\mathcal{C}', \mathcal{C}} \sqrt{p^0(\mathcal{C})}$ where

$$\hat{H}_i(\nu) = \hat{n}_{i-1} [\sqrt{c(1-c)}(\sigma_i^- + \sigma_i^+) - (1-\nu)(1-2c)\hat{n}_i - (1-\nu)c] \quad (\text{A.1})$$

is a symmetric (self-adjoint) operator associated with flips of spin i . Since the trial potentials that we consider are translationally invariant along the chain, (35) becomes

$$F = \frac{-\sum_{\mathcal{C}, \mathcal{C}'} \sqrt{\tilde{p}(\mathcal{C}')} [\hat{H}_i(\nu)]_{\mathcal{C}', \mathcal{C}} \sqrt{\tilde{p}(\mathcal{C})}}{\sum_{\mathcal{C}} \tilde{p}(\mathcal{C})} \quad (\text{A.2})$$

where $[\hat{H}_i(\nu)]_{\mathcal{C}', \mathcal{C}}$ indicates a matrix element of $\hat{H}_i(\nu)$. It is convenient to write the numerator here as $\sum_{\mathcal{C}, \mathcal{C}'} O_i(\mathcal{C}, \mathcal{C}') \tilde{p}(\mathcal{C})$, with

$$O_i(\mathcal{C}', \mathcal{C}) = \sqrt{\frac{\tilde{p}(\mathcal{C}')}{\tilde{p}(\mathcal{C})}} [\hat{H}_i(\nu)]_{\mathcal{C}', \mathcal{C}}. \quad (\text{A.3})$$

We note (i) that $O_i(\mathcal{C}', \mathcal{C}) = 0$ unless \mathcal{C} and \mathcal{C}' coincide for all spins j except $j = i$, and (ii) that $O_i(\mathcal{C}', \mathcal{C})$ depends only on spins $n_{i-B+1}, \dots, n_{i+B-1}$ (as long as $B > 1$). One may therefore use the transfer matrix representation of \tilde{p} to sum over all spins n'_j except for $j = i$, and over all spins n_j with $j < i - B + 1$ or $j > i + B - 1$. The result (for a periodic chain of length L) is

$$F_B = \frac{1}{\text{tr}(M^L)} \sum_{n'_i} \sum_{n_{i-B+1}, \dots, n_{i+B-1}} O(\mathcal{C}, \mathcal{C}') \left[\prod_{j=i-B+1}^{i-1} M_{\mathcal{B}_j, \mathcal{B}_{j+1}} \right] (M^{L-B+1})_{\mathcal{B}_i, \mathcal{B}_{i-B+1}} \quad (\text{A.4})$$

For long chains, the matrix element $(M^{L-B+1})_{\mathcal{B}, \mathcal{B}'}$ can be replaced by $\lambda_{\max}^{L-B+1} x(\mathcal{B}) y(\mathcal{B}')$ where λ_{\max} is the largest eigenvalue of M and x and y the corresponding right and left eigenvectors. The resulting expression may therefore be evaluated by constructing and diagonalising M . After minimising F over the variational parameters $z_{\mathcal{B}}$, one may then evaluate any one-time observable in the ν -ensemble, via the transfer matrix M .

Appendix A.2. Exponential decay of domain distribution in the block model

Here, we outline a derivation that shows that if the effective potential of a system is a block model of range B then distributions of domain sizes decay exponentially for ranges $r > B$. For systems described by a block model, the probability of observing a block in state \mathcal{B} is

$$P(\mathcal{B}) = \frac{\text{tr}(M^N e^{\mathcal{B}})}{\text{tr}(M^N)} \quad (\text{A.5})$$

where M is the transfer matrix of the previous section, and $e^{\mathcal{B}}$ is a diagonal matrix with $e_{\mathcal{B}, \mathcal{B}} = 1$ and all other entries being zero. Assuming that the matrix M has a gap between its largest and second largest eigenvalues then for very large N , $M^N \approx \mathbf{v} \lambda^N \mathbf{u}^T$ where λ is the largest eigenvalue of M and \mathbf{u}, \mathbf{v} the associated left and right eigenvectors, normalised such that $\mathbf{u} \cdot \mathbf{v} = 1$. Hence, as $N \rightarrow \infty$, one has $P(\mathcal{B}) \rightarrow v_{\mathcal{B}} u_{\mathcal{B}}$.

Further, the probability that blocks i and $i + 1$ are in states $\mathcal{B}, \mathcal{B}'$ is

$$P(\mathcal{B}, \mathcal{B}') = \frac{\text{tr}(M^{N-1} e^{\mathcal{B}} M e^{\mathcal{B}'})}{\text{tr}(M^N)} \quad (\text{A.6})$$

Again, for large N the trace is dominated by the largest eigenvalue of M , so that $P(\mathcal{B}, \mathcal{B}') \rightarrow u_{\mathcal{B}} M_{\mathcal{B}, \mathcal{B}'} v_{\mathcal{B}'} / \lambda$. Finally, the analogous property for three successive blocks (for $N \rightarrow \infty$) is easily shown to be $P(\mathcal{B}, \mathcal{B}', \mathcal{B}'') \rightarrow u_{\mathcal{B}} M_{\mathcal{B}, \mathcal{B}'} M_{\mathcal{B}', \mathcal{B}''} v_{\mathcal{B}''} / \lambda^2$ from which we can read off that

$$P(\mathcal{B}, \mathcal{B}', \mathcal{B}'') = \frac{P(\mathcal{B}, \mathcal{B}') P(\mathcal{B}', \mathcal{B}'')}{P(\mathcal{B}')} \quad (\text{A.7})$$

Recalling that specifying three successive blocks determines the configuration of $B+2$ successive spins, consider the probability of finding these spins in the configuration $(n_i, 0^B, n_{i+B+1})$, where 0^B stands for B successive down spins. From (A.7), this is seen to be

$$P(n_i, 0^B, n_{i+B+1}) = \frac{P(n_i, 0^B) P(0^B, n_{i+B+1})}{P(0^B)}, \quad (\text{A.8})$$

and generalising to more than three blocks leads to the more general formula

$$P(n_i, 0^{B+x}, n_{i+B+x+1}) = \frac{P(n_i, 0^B) P(0^{B+1})^x P(0^B, n_{i+B+x+1})}{P(0^B)^{x+1}}. \quad (\text{A.9})$$

Finally, identifying the domain size distribution $p(d) = P(1, 0^{d-1}, 1)/P(1)$, one sees that $p(d)$ decays exponentially for $d > B$, proportional to $[P(0^{B+1})/P(0^B)]^{d-B}$. A similar result is familiar for the domain structure in one-dimensional Ising systems: in that case $B = 2$, and we note that our definition of $p(d)$ is then directly related to the distribution of sizes of spin-down domains.

Appendix A.3. Variational free energy for p_d -model

The calculation of the variational free energy for the p_d -model also relies on properties of the matrix element $O_i(\mathcal{C}, \mathcal{C}')$ given in (A.3). Since $O_i(\mathcal{C}', \mathcal{C}) \neq 0$ only if $n_{i-1} = 1$, one should consider only configurations \mathcal{C} where a ‘domain’ starts at site $i - 1$. This occurs with probability $\langle n_{i-1} \rangle^{\text{var}} = \frac{1}{\sum d p_d}$ where we use the notation $\langle \cdot \rangle^{\text{var}}$ for averages with respect to the trial distribution \tilde{p} . Recalling in addition that $O_i(\mathcal{C}', \mathcal{C}) = 0$ unless either $\mathcal{C} = \mathcal{C}'$ or \mathcal{C}' and \mathcal{C} differ only at spin i , one finds that $O_i(\mathcal{C}', \mathcal{C})$ depends on the size d of the domain starting at site $i - 1$; if $d > 1$ then it depends only on d while if $d = 1$ then $O_i(\mathcal{C}', \mathcal{C})$ also depends on the size of domain d' that starts at i . Identifying the relevant cases leads directly from (A.2) to (38).

Appendix A.4. Variational free energy for the p_{fe} -model

Within the p_{fe} model, the variational free energy is calculated similarly to the p_d model. The probability that spin $i - 1$ occupies a particular position within a domain of parameters (f, e) is $p_{fe} / \sum_{f'e'} (f' + e') p_{f'e'}$. The matrix element $O_i(\mathcal{C}, \mathcal{C}') \neq 0$ only if spin $i - 1$ is one of the f up spins in this domain. The derivation of the variational free energy then follows that for the p_d model, except that it requires an additional explicit summation over the f possible positions of spin $i - 1$ within the domain. The matrix element $O_i(\mathcal{C}, \mathcal{C}')$ depends only on the domain containing site $i - 1$, except in the case that this domain has $e = 1$, in which case it depends additionally on the next domain to the right. Enumerating the specific cases, one arrives at (40).

References

- [1] H. Touchette, Phys. Rep. **478**, 1 (2009).
- [2] D. Ruelle, “*Thermodynamic Formalism*” (Addison-Wesley, Reading, 1978); J.-P. Eckmann and D. Ruelle, Rev. Mod. Phys. **57** (1985), 617.
- [3] G. Gallavotti and E. G. D. Cohen, J. Stat. Phys. **80** (1995), 931; C. Jarzynski, Phys. Rev. Lett. **78** (1997), 2690; J. Kurchan, J. Phys. A **31** (1998), 3719; J.L. Lebowitz and H. Spohn, J. Stat. Phys. **95** (1999), 333; C. Maes, J. Stat. Phys. **95** (1999), 367; G. E. Crooks, Phys. Rev. E **61** (2000), 2361.
- [4] L. Bertini, A. De Sole, D. Gabrielli, G. Jona-Lasinio and C. Landim, J. Stat. Phys. **135** (2009), 857.

- [5] T. Bodineau and B. Derrida, Phys. Rev. Lett. **92** (2004), 180601.
- [6] D. Simon, J. Stat. Mech. (2009) P07017.
- [7] A. Imparato, V. Lecomte and F. van Wijland, Phys. Rev. E **80**, 011131 (2009)
- [8] V. Popkov, G. M. Schütz, and D. Simon, J. Stat. Mech. (2010), P10007; V. Popkov and G. M. Schütz, J. Stat. Phys. **142**, 627 (2011).
- [9] R. M. L. Evans, Phys. Rev. Lett. **92**, 150601 (2004); J. Phys. A **38**, 293 (2005).
- [10] J. P. Garrahan, R. L. Jack, V. Lecomte, E. Pitard, K. van Duijvendijk and F. van Wijland, Phys. Rev. Lett. **98**, 195702 (2007); J. Phys. A **42**, 075007 (2009).
- [11] L. O. Hedges, R. L. Jack, J. P. Garrahan and D. Chandler, Science **323**, 1309 (2009).
- [12] R. L. Jack and J. P. Garrahan, Phys. Rev. E **81**, 011111 (2010).
- [13] Y. S. Elmatad, R. L. Jack, J. P. Garrahan and D. Chandler, PNAS **107**, 12793 (2010).
- [14] C. Maes and M. H. Wieren, Phys. Rev. Lett. **96**, 240601 (2006).
- [15] V. Lecomte, C. Appert-Roland and F. van Wijland, Phys. Rev. Lett. **95**, 010601 (2005); J. Stat. Phys. **127**, 51 (2007).
- [16] A. Baule and R. M. L. Evans, Phys. Rev. Lett. **101**, 240601 (2008).
- [17] A. Simha and R. M. L. Evans, Phys. Rev. E **77**, 031117 (2008).
- [18] R. L. Jack and P. Sollich, Prog. Theor. Phys. Supp. **184**, 304 (2010)
- [19] A. Baule and R. M. L. Evans, J. Stat. Mech. (2010), P03030.
- [20] R. Chetrite and H. Touchette, Phys. Rev. Lett. **111**, 120601 (2013).
- [21] R. L. Jack, L. O. Hedges, J. P. Garrahan and D. Chandler, Phys. Rev. Lett. **107**, 275702 (2011).
- [22] T. Speck, A. Malins and C. P. Royall, Phys. Rev. Lett. **109**, 195703 (2012)
- [23] J. Jäckle and S. Eisinger, Z. Phys. B **84**, 115 (1991).
- [24] F. Ritort and P. Sollich, Adv. Phys. **52**, 219 (2003).
- [25] J. P. Garrahan, P. Sollich and C. Toninelli, Ch. 10 in *Dynamical heterogeneities in glasses, colloids and granular media*, eds: L. Berthier, G. Biroli, J.-P. Bouchaud, L. Cipelletti and W. van Saarloos (OUP, Oxford UK).
- [26] P. Sollich and M. R. Evans, Phys. Rev. Lett. **83**, 3238 (1999); Phys. Rev. E **68**, 031504 (2003).
- [27] D. Aldous and P. Diaconis, J. Stat. Phys. **107**, 945 (2002).
- [28] N. Cancrini, F. Martinelli, C. Roberto and C. Toninelli, J. Stat. Mech. (2007) L03001
- [29] D. Chandler and J. P. Garrahan, Ann. Rev. Phys. Chem. **61**, 191 (2010); J. P. Garrahan and D. Chandler, Phys. Rev. Lett. **89**, 035704 (2002); L. Berthier and J. P. Garrahan, J. Phys. Chem. B **109**, 3578 (2005); Y. S. Elmatad, D. Chandler and J. P. Garrahan, J. Phys. Chem. B **113**, 5563 (2009).
- [30] To make this approximate scaling relation precise, one may define $\pi_K(k) = \lim_{N \rightarrow \infty} \lim_{t_{\text{obs}} \rightarrow \infty} (-N t_{\text{obs}})^{-1} \ln P_0(N t_{\text{obs}} k)$: the order and existence of the limits is discussed, for example, in [10].
- [31] More precisely, $(-N t_{\text{obs}})^{-1} \ln \langle e^{-sK} \rangle_0 \rightarrow \psi_K(s)$ as $N, t_{\text{obs}} \rightarrow \infty$: the relation is analogous to that between $P_0(K)$ and $\pi_K(k)$.
- [32] M. Merolle, J.P. Garrahan and D. Chandler, Proc. Natl. Acad. Sci. USA **102** (2005), 10837.
- [33] Y. S. Elmatad and R. L. Jack, J. Chem. Phys. **138**, 12A531 (2013).
- [34] C. Maes, F. Redig and A. van Moffaert, J. Stat. Phys. **96**, 69 (1999)
- [35] A. C. D. van Enter, R. Fernández and A. D. Sokal, J. Stat. Phys. **72**, 879 (1993)
- [36] P. Bolhuis, D. Chandler, C. Dellago, and P. Geissler, Ann. Rev. Phys. Chem. **53**, 291 (2002).
- [37] R. L. Jack, J. P. Garrahan and D. Chandler, J. Chem. Phys. **125**, 184509 (2006).
- [38] A. Widmer-Cooper, P. Harrowell and H. Fynewever, Phys. Rev. Lett. **93** 135701 (2004).
- [39] R. L. Jack, arXiv:1309.6247.
- [40] M. Gorrissen, J. Hooyberghs and C. Vanderzande, Phys. Rev. E **79**, 020101(R) (2009).
- [41] U. Schollwöck, Ann. Phys. **326**, 96 (2011).